V.A. Romaka *doc. tech. Science, professor*[1],
Yu.V. Stadnyk *cand. chem. Science*[2],
L.P. Romaka *cand. chem. Science*[2],
V.Z. Pashkevych *cand. tehn., docent*[1],
V.V. Romaka *doc. tech. Science*[3],
A.M. Horyn *cand. chem. Science*[2],
P.Yu. Demchenko *cand. chem. Science*[2]

[1]National University "Lvivska Politechnika", 12,
S. Bandera Str., Lviv, 79013, Ukraine, *e-mail: vromaka@polynet.lviv.ua*;
[2]Ivan Franko National University of Lviv, 6, Kyryla and Mefodiya Str.,
Lviv, 79005, Ukraine, *e-mail: lyubov.romaka@lnu.edu.ua*;
[3]Technische Universität Dresden, Bergstrasse 66,
01069 Dresden, Germany, *e-mail: vromakal@gmail.com*

STUDY OF STRUCTURAL, THERMODYNAMIC, ENERGY, KINETIC AND MAGNETIC PROPERTIES OF THERMOELECTRIC MATERIAL $Lu_{1-x}Zr_xNiSb$

The crystal and electronic structures, thermodynamic, kinetic, energy and magnetic properties of the thermoelectric material $Lu_{1-x}Zr_xNiSb$ in the ranges: T=80–400 K, x=0–0.10 were studied. Mechanisms of simultaneous generation of structural defects of acceptor and donor nature are established. It is shown that in the structure of the basic compound LuNiSb there are defects of acceptor nature as a result of vacancies in the crystallographic positions 4a and 4c of Lu and Ni atoms, respectively, which gave rise to acceptor levels (zones) in the band gap ε_g. Introduction of Zr impurity atoms into the structure of the LuNiSb compound by substitution of Lu atoms in position 4a generates structural defects of donor nature with simultaneous elimination of vacancies in positions 4a and 4c of Lu and Ni atoms, respectively (acceptor levels). The ratio of the concentrations of the available defects of donor and acceptor nature determines the location of the Fermi level ε_F and the conduction mechanisms in $Lu_{1-x}Zr_xNiSb$. The investigated solid solution $Lu_{1-x}Zr_xNiSb$ is a promising thermoelectric material. Bibl. 15, Fig. 9.

Keywords: electronic structure, electrical resistivity, thermopower coefficient.

Introducion

A new promising class of semiconductor thermoelectric materials with high efficiency of conversion of thermal energy into electricity are solid substitution solutions based on *RNiSb* compounds (*R* – rare earth metals of the yttrium subgroup) [1 – 4], which crystallize in the structural type *MgAgAs* (sp. group $F\bar{4}3m$) [5]. Thus, in [1 – 6], when studying the structural, kinetic and magnetic characteristics of *RNiSb* compounds, it was found that their crystal structure is defective, and the compounds themselves are semiconductors of the hole-type conductivity. Thus, in the crystal there is a mechanism for generating structural defects of acceptor nature. However, today there is no model of the structure of *RNiSb* and the mechanism of generating defects, which are adequate to the results of the experiment.

It is known that one of the ways to obtain thermoelectric materials with high values of thermoelectric quality factor Z is to generate in the crystal structural defects of donor and/or acceptor nature, which simultaneously leads to changes in the values of thermopower coefficient $\alpha(T, x)$ and thermal conductivity $\kappa(T, x)$, as well as the specific conductivity $\sigma(T, x)$ [7]. Therefore, to obtain a new thermoelectric material, a semiconductor solid solution of $Lu_{1-x}Zr_xNiSb$ obtained by doping a *LuNiSb* compound with *Zr* atoms by substituting *Lu* atoms at the crystallographic position 4*a* was investigated. In this case, structural defects of donor nature must be generated in the semiconductor, because the *Zr* atom ($4d^25s^2$) has a larger number of *d*-electrons than *Lu* ($5d^16s^2$).

On the other hand, without knowing the features of the spatial arrangement of atoms in *RNiSb* compounds and, in particular, in *LuNiSb*, it is almost impossible to understand the mechanism of entry of impurity atoms into the semiconductor matrix when obtaining a suitable solid solution. And this makes it unpredictable to obtain thermoelectric material with high values *Z*. Thus, the authors [4, 6] based on the results of calculating the density distribution of electronic states DOS *LuNiSb* for different variants of atoms in the nodes of the unit cell and the degree of occupancy of positions of own and/or foreign atoms suggested the existence of vacancies (~6%) in position 4*c* atoms *Ni*. In this case, structural defects of acceptor nature are generated in the crystal, and acceptor levels (zone) ε_A^1 appear in the band gap ε_g, which corresponds to the results of the experiment [6].

The following results of the study of structural, thermodynamic, kinetic, energy and magnetic characteristics of the semiconductor solid solution $Lu_{1-x}Zr_xNiSb$, $x = 0 – 0.10$, will clarify the crystal and electronic structure of the basic semiconductor *LuNiSb*. This will allow us to understand both the nature of *LuNiSb* defects and make the process of optimizing the characteristics of the thermoelectric material $Lu_{1-x}Zr_xNiSb$ predictable.

Research methods

The crystal structure, the distribution of the density of electronic states (DOS), and the magnetic, thermodynamic, kinetic, and energy characteristics of $Lu_{1-x}Zr_xNiSb$ have been studied. Samples of the solid solution $Lu_{1-x}Zr_xNiSb$ were synthesized by fusing the charge of the initial components in an electric arc furnace in an inert argon atmosphere followed by homogenizing annealing for 720 h at a temperature of 1073 K. Crystallographic parameters were calculated using the program Fullprof [8]. Diffraction data arrays were obtained using a powder diffractometer STOE STADI P ($Cu\mathrm{K}\alpha_1$ radiation).. Calculations of the electronic structure, density distribution of electronic states (DOS), electron localization function (ELF), thermodynamic characteristics, as well as optimization of the crystal structure parameters of the $Lu_{1-x}Zr_xNiSb$ thermoelectric material were performed using the Koringa-Kon-Rostoker method as a method. Kohn-Rostoker (hereinafter KKR) in the Coherent Potential Approximation (CPA) and Local Density Approximation (LDA) approximation, as well as the Full Potential Linearized Augumented Plane Waves (FLAPW) method. KKR simulations were performed using AkaiKKR software packages [9] in the local density approximation for the exchange-correlation potential with parameterization Moruzzi, Janak, Williams (MJW) [10] in the semi-relativistic consideration of the core level and spin-orbit interaction. For calculations using the FLAPW method used in the software package Elk [11]. The simulation was performed for a 10×10×10 *k*-grid in both the local density (LDA) and generalized GGA gradient approximations. The Brillouin zone was divided into 1000 *k*-points, which were used to calculate the Bloch spectral function (band energy spectrum) and the density of electronic states. The width of the energy window was chosen so as to capture the semi-core states of *p*-elements. Visualization of volumetric data was performed using the program VESTA [12]. Topological analysis and interpretation of DOS and ELF were performed within the framework of Bader's theory [13]. The accuracy of calculations of the position

of the Fermi level $\varepsilon_F \pm 6$ meV. Temperature and concentration dependences of resistivity (ρ) and thermopower coefficient (α) with respect to copper and magnetic susceptibility (χ) (Faraday method) of $Lu_{1-x}Zr_xNiSb$ samples, $x = 0 – 0.10$, in the temperature range $T = 80 – 400$ K were measured.

Investigation of structural characteristics of $Lu_{1-x}Zr_xNiSb$

Microprobe analysis of the concentration of atoms on the surface of $Lu_{1-x}Zr_xNiSb$ samples established their correspondence to the initial compositions of the charge, and *X*-ray phase and structural analyzes showed that the diffraction patterns of samples including $x = 0 – 0.1$ are indexed in the structural type of *MgAgAs* [5] phases (Fig. 1*a*). With the help of structural studies, the change in the values of the period of the unit cell $a(x)$ $Lu_{1-x}Zr_xNiSb$ was established. Since the atomic radius *Lu* ($r_{Lu} = 0.173$ nm) is larger than *Zr*/($r_{Zr} = 0.160$ nm), it was logical to expect a decrease in the values of the period of the unit cell $a(x)$ when substituting Lu atoms at position 4*a* for *Zr* atoms. In this case, as mentioned above, structural defects of donor nature will be generated in the crystal, and impurity donor levels (zone) ε_D^1 will appear in the forbidden zone ε_g.

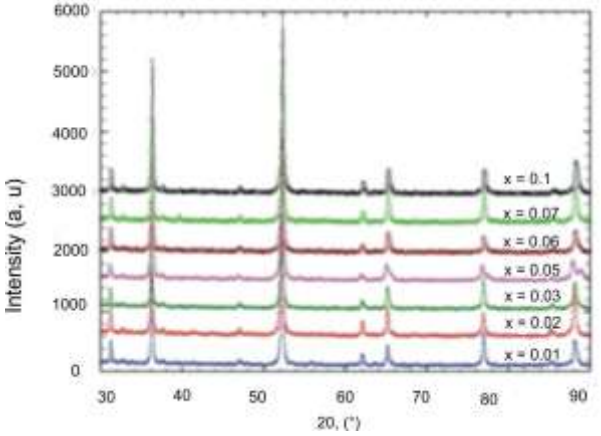

a)

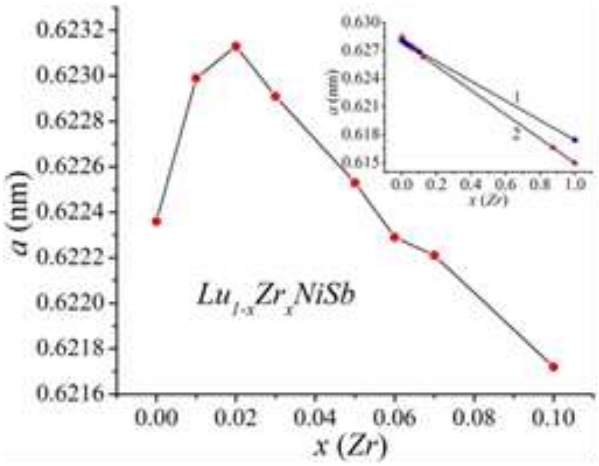

b)

Fig. 1. Diffractograms of samples (a) and change of values of the period of the unit cell a(x) (b) $Lu_{1-x}Zr_xNiSb$; insert: simulation a(x): 1 – using the program AkaiKKR, 2 – the program Elk

However, the results of the structural analysis of $Lu_{1-x}Zr_xNiSb$ show (Fig. 1*b*) that in the area of concentrations $x = 0 – 0.02$ the values of the period $a(x)$ increase rapidly, pass through the maximum and decrease just as rapidly at $x > 0.02$. In a related semiconductor solid solution $Er_{1-x}Zr_xNiSb$, we observed a similar behavior of the period of the unit cell $a(x)$: in the region $x = 0 – 0.02$ the values of $a(x)$ increased, and at concentrations $x > 0.05$ decreased [3].

The fact that in $Lu_{1-x}Zr_xNiSb$ there is a nonmonotonic change in the values of the period of the unit cell $a(x)$ (Fig. 1*b*) suggests that impurity *Zr* atoms introduced into the matrix of *LuNiSb* compounds not only replace *Lu* atoms in position 4*a*, but can also partially occupy both different crystallographic positions and generate the appearance of atoms in the tetrahedral voids of the structure, which make up ~24% of the volume of the unit cell [6].

Formally, based on geometric considerations, we can assume that the increase in the values of the period of the unit cell $a(x)$ $Lu_{1-x}Zr_xNiSb$ could cause partial occupation of the crystallographic position of 4*c Ni* atoms by *Zr* atoms. After all, the atomic radius of the Ni atom ($r_{Ni} = 0.124$ nm) is the smallest among the chemical elements $Lu_{1-x}Zr_xNiSb$ ($r_{Sb} = 0.159$ nm). However, such an assumption is unlikely due to the significant difference in the atomic radii of *Zr* and *Ni*. On the other hand, there is a high probability of returning *Ni* atoms to position 4*c* (filling vacancies of the *LuNiSb* compound [4, 6]), which can lead to an increase in the values of $a(x)$ and the elimination of vacancies. We also do not rule out the presence of vacancies in the crystallographic position 4*a*, which also generates structural defects of acceptor nature. The occupation of these vacancies by impurity *Zr* atoms also generates the appearance of structural defects of donor nature and leads to an increase in the values of $a(x)$ $Lu_{1-x}Zr_xNiSb$. However, the accuracy of *X*-ray structural studies does not allow to experimentally identify these vacancies.

Therefore, from the results of experimental results it follows that in the structure of $Lu_{1-x}Zr_xNiSb$ the following processes can occur simultaneously:

– substitution at position 4*a* of *Lu* atoms by *Zr* atoms, which generates structural defects of donor nature in the crystal and the appearance of donor levels (zone) ε_D^1 in the band gap ε_g;

– return of *Ni* atoms to position 4*c* and elimination of vacancies generates defects of donor nature, and impurity donor levels (zones) of ε_D^2 will appear in the forbidden zone. At the same time, the vacancy disappears and in the forbidden zone εg the corresponding acceptor level (zone) ε_A^1.

– occupation of vacancies in position 4*a* by *Zr* atoms simultaneously eliminates the structural defect of acceptor nature and now generates a defect of donor nature with the appearance of the corresponding donor level (zone) ε_D^3 in the forbidden zone ε_g.

To better understand the structural transformations in $Lu_{1-x}Zr_xNiSb$, we calculated the change in the values of the period of the unit cell $a(x)$ $Lu_{1-x}Zr_xNiSb$ using the software packages AkaiKKR [9] and Elk [11] (Fig. 1*b*, insert). The results of the calculation of the change in $a(x)$ $Lu_{1-x}Zr_xNiSb$ by both methods, in contrast to the experimental results, show only a monotonic decrease in the values of the cell period, which is quite logical and predictable provided that only *Lu* atoms are replaced by *Zr*.

From the insert of fig. 1*b* also shows that the values of the period of the unit cell of the *LuNiSb* compound, obtained by simulation by the software package AkaiKKR [9], are less than those obtained by implementing the software package Elk [11]. At the same time, the simulation result for the hypothetical compound *ZrNiSb* (the other side of the solid solution $Lu_{1-x}Zr_xNiSb$ for x=1) showed the opposite result: the values of period a of the compounds *ZrNiSb* obtained by AkaiKKR [9] are greater than those obtained by Elk [11]. Therefore, the course of the dependences $a(x)$ $Lu_{1-x}Zr_xNiSb$, obtained by different modeling methods, occurs according to different laws. In this case, the angles of inclination of the dependences $a(x)$ $Lu_{1-x}Zr_xNiSb$ are different. It turned out that the angle of change of the values of the period of the cell $a(x)$ $Lu_{1-x}Zr_xNiSb$, obtained from the experiment, coincides with that when using the software package Elk [11]. This result indicates a higher accuracy of modeling the structural characteristics of $Lu_{1-x}Zr_xNiSb$ by the FLAPW method compared to the KKR method.

Investigation of thermodynamic characteristics of $Lu_{1-x}Zr_xNiSb$

Based on the fact that there is no *ZrNiSb* compound with the structure of *MgAgAs*, and hence 100 % substitution of *Lu* atoms for *Zr* and vice versa, it is important to establish the limits of the possible existence of a solid solution of $Lu_{1-x}Zr_xNiSb$. For this purpose, modeling of thermodynamic characteristics for a hypothetical solid solution $Lu_{1-x}Zr_xNiSb$, $x = 0 – 1.0$, in the approximation of harmonic oscillations of atoms in the framework of the DFT density functional theory was performed. The change in the values of the enthalpy of mixing ΔH (Fig. 2*a*) and the total energy ΔE (Fig. 2*b*) $Lu_{1-x}Zr_xNiSb$, $x = 0 – 1.0$, suggests that the thermoelectric material exists as a solid substitution solution in the concentration range $x < 0.20$.

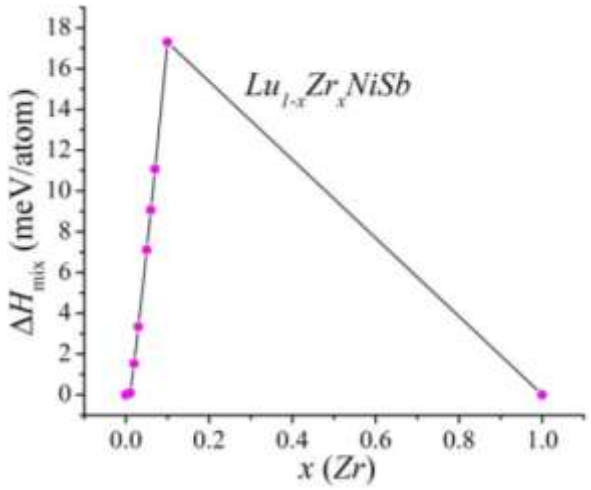

a)

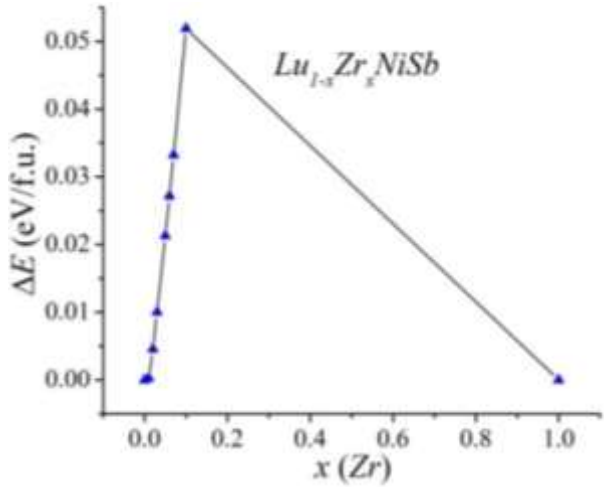

b)

Fig. 2. Calculation by Elk method of change of enthalpy values of mixing ΔH (a) and total energy ΔE (b) of solid solution $Lu_{1-x}Zr_xNiSb$

In this concentration region, the values of the enthalpy of mixing $\Delta H(x)$ and the total energy $\Delta E(x)$ increase, indicating the energy expediency of substituting *Lu* atoms for *Zr*. However, at higher concentrations of impurity atoms *Zr*, $x > 0.20$, the dependences $\Delta H(x)$ and $\Delta E(x)$ decrease, which indicates

the energy disadvantage of the formation of a solid substitution solution. Stratification (spinoidal phase decay) occurs and thermoelectric material does not exist. Therefore, the region of existence of the solid substitution solution $Lu_{1-x}Zr_xNiSb$ is limited by the concentration $x = 0.20$.

Investigation of electrokinetic and energy characteristics of $Lu_{1-x}Zr_xNiSb$

Temperature and concentration dependences of specific electrical resistance ρ and thermopower coefficient α of samples $Lu_{1-x}Zr_xNiSb$, $x = 0 – 0.10$, are shown in Fig. 3 – 7.

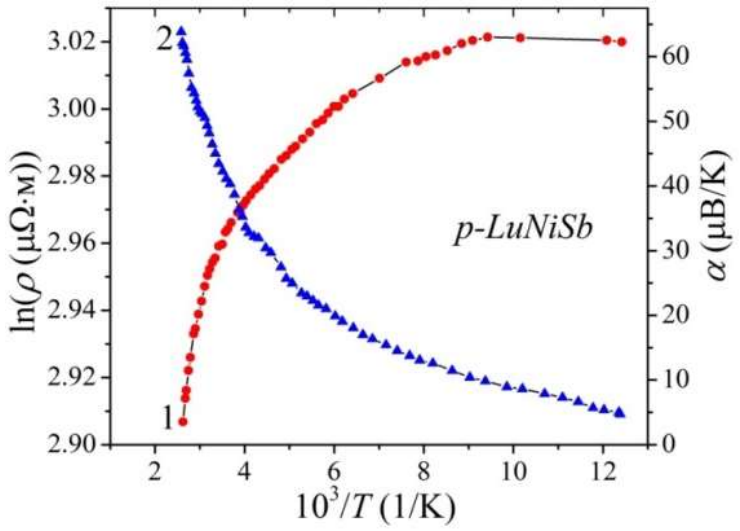

a)

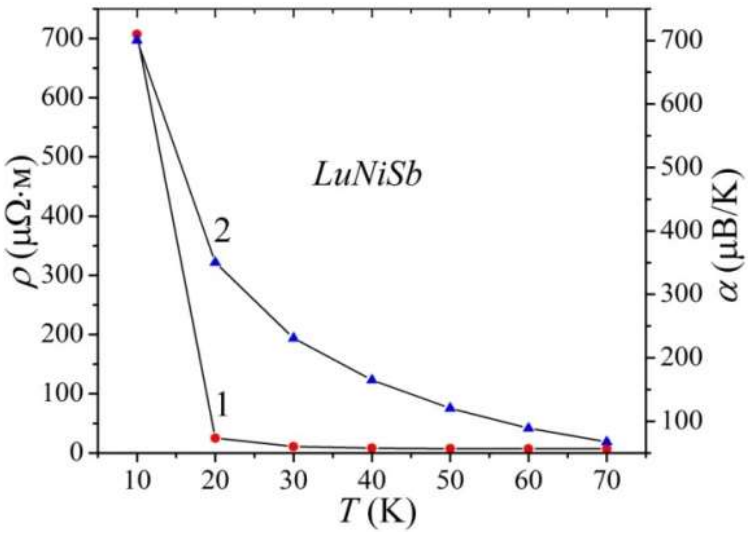

b)

Fig. 3. Temperature dependences of specific electrical resistance ρ (1) and thermo-emf coefficient α (2) LuNiSb; a – the results of the experiment, b – the calculation in the range T = 4.2–70 K

As we can see from Fig. 3, for the basic compound *LuNiSb* the dependence ln(ρ(1/*T*)) is characteristic of semiconductors [14] and is approximated by the known relation (1):

$$\rho^{-1}(T) = \rho_1^{-1} \exp\left(-\frac{\varepsilon_1^{\rho}}{k_B T}\right) + \rho_3^{-1} \exp\left(-\frac{\varepsilon_3^{\rho}}{k_B T}\right), \quad (1)$$

where the first high-temperature term describes the activation of current carriers ε_1^{ρ} from the Fermi level ε_F to the level of continuous energy zones, and the second, low-temperature term, the hopping conductivity at impurity donor states ε_3^{ρ} with energies close to the Fermi level ε_F. Calculations showed that in the *p-LuNiSb* semiconductor the Fermi level ε_F is located at a distance ε_1^{ρ} = 10.2 meV from the ceiling of the valence band ε_V.

Temperature dependences of the thermopower coefficient α(1/*T*) *p-LuNiSb* (Fig. 3*a*) are described by the known expression (2) [15]:

$$\alpha = \frac{k_B}{e}\left(\frac{\varepsilon_i^{\alpha}}{k_B T} - \gamma + 1\right), \quad (2)$$

where γ is a parameter that depends on the nature of the scattering mechanism. From the high- and low-temperature activation regions of the α(1/*T*) dependence, the values of activation energies ε_1^{α} = 35.3 meV and ε_3^{α} = 1.9 meV were calculated, which, as shown in [6], are proportional to the amplitude of large-scale fluctuations of continuous energy and small-scale zones. of fluctuations of strongly doped and highly compensated semiconductor [14].

The presence of a high-temperature activation region on the temperature dependence of the resistivity ln(ρ(1/*T*)) *p-LuNiSb* indicates the location of the Fermi level ε_F in the band gap ε_g of the semiconductor, and positive values of the thermopower coefficient α(*T*) at these temperatures specify its position – near the valence band ε_V. Therefore, holes are the main carriers of electric current. The obtained values of activation energies ε_1^{ρ} and ε_1^{α} for *p-LuNiSb* are consistent with the results of previous studies [4, 6].

Modeling of temperature dependences of kinetic characteristics of *LuNiSb* compound in the temperature range *T* = 4.2 – 70 K shows a rapid decrease in the values of resistivity ρ(*T*) in the range *T* = 4.2 – 20 K (Fig. 3*b*). This behavior ρ(*T*) is characteristic of semiconductors when there is an increase in the number of free current carriers due to their activation from the Fermi level ε_F. Such carriers are holes, which is indicated by positive values of the thermo-emf coefficient α(*T*) *LuNiSb*, and this is consistent with the results of the experiment.

The introduction of *Zr* atoms into the structure of the *LuNiSb* compound by substituting *Lu* atoms at position 4*a* generates structural defects of donor nature in $Lu_{1-x}Zr_xNiSb$. Simulation of the change in the values of resistivity ρ(*x*,*T*) at the lowest concentration of *Zr* atoms (*x* = 0.01) shows two fundamentally different areas: at temperatures *T* = 4.2 – 20 K, the values of ρ(*T*) decrease, which is characteristic of semiconductors, and with increasing temperatures – increase, indicating the metallic type of conductivity (Fig. 4). The values of the thermopower coefficient α(*T*) $Lu_{0.99}Zr_{0.01}NiSb$ decrease rapidly from the values of $\alpha_{4.2\ K}$ = 225 μV/K to $\alpha_{70\ K}$ = -20 μV/K. The change in the sign of the thermopower coefficient α(*T*) indicates a change in the type of conductivity when the main current carriers are electrons. The Fermi level ε_F is located in the conduction band ε_C.

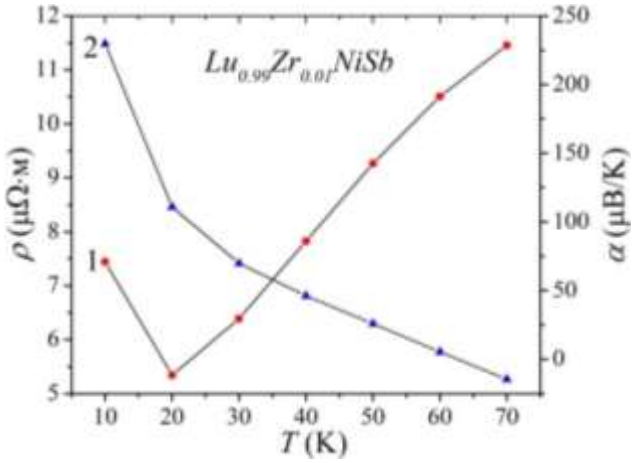

a)

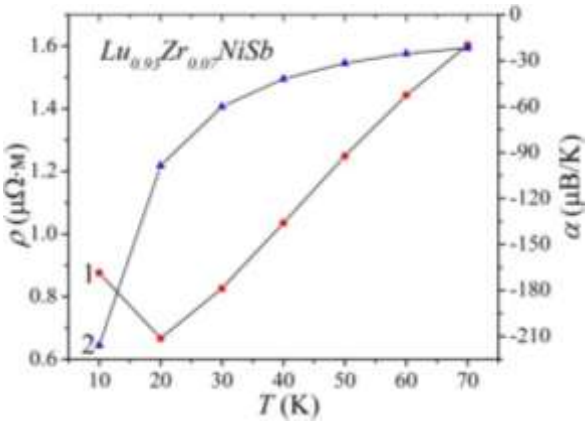

b)

Fig. 4. Results of modeling the temperature dependences of the resistivity ρ (T, x) (1) and the thermo-emf coefficient α (T, x) (2) Lu1-xZrxNiSb at temperatures T = 4.2–70

At an even higher concentration of *Zr* atoms ($x = 0.07$ and $x = 0.10$) in the temperature range $T = 4.2 – 70$ K, the sign of the thermopower coefficient $\alpha(T)$ remains negative, and the nature of the change in resistivity values $\rho(T)$ is similar, as for the case when the concentration of *Zr* atoms was $x = 0.01$ (Fig. 4). The fact that at all concentrations of *Zr* atoms in the temperature range $T = 4.2 – 20$ K the values of the resistivity $\rho(T,x)$ $Lu_{1-x}Zr_xNiSb$ decrease indicates the depth of occurrence in the band gap ε_g of the donor states. At low temperatures ($T < 20$ K), the thermal energy is insufficient for the activation of electrons in the conduction band ε_C. However, at temperatures $T > 20$ K the concentration of free electrons becomes significant and the Fermi level ε_F enters the conduction band ε_C, indicating the transition of the conductivity of the dielectric metal, which is the Anderson transition [15].

Doping *p-LuNiSb* with the smallest in the experiment concentration of *Zr* atoms ($x = 0.01$) radically changes both the nature of the behavior of temperature dependences of resistivity $\rho(T, x)$ and the thermopower coefficient $\alpha(T,x)$, and the type of main carriers of electric current (Fig. 5*a*, 6*a*). The metallic nature of the behavior of the temperature dependences of the resistivity $\rho(T, x)$ $Lu_{1-x}Zr_xNiSb$ (Fig. 5*a*) indicates that the Fermi level ε_F has left the band gap ε_g and is in the zone of continuous energies. The fact

that such a zone is a conduction band ε_C can be stated on the basis of negative values of the thermopower coefficient $\alpha(T, x)$ (Fig. 6*a*) at all concentrations and temperatures. It is clear that the increase in the values of $\rho(T, x)$ $Lu_{1-x}Zr_xNiSb$ with increasing temperature is due to the current carriers in the semiconductor scattering mechanisms.

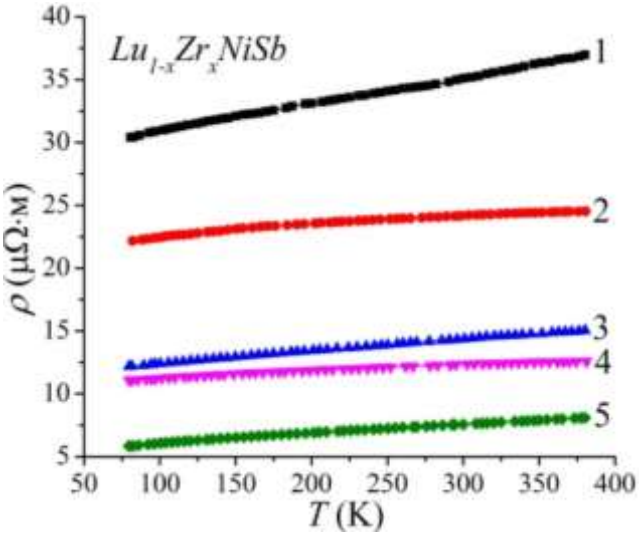

a)

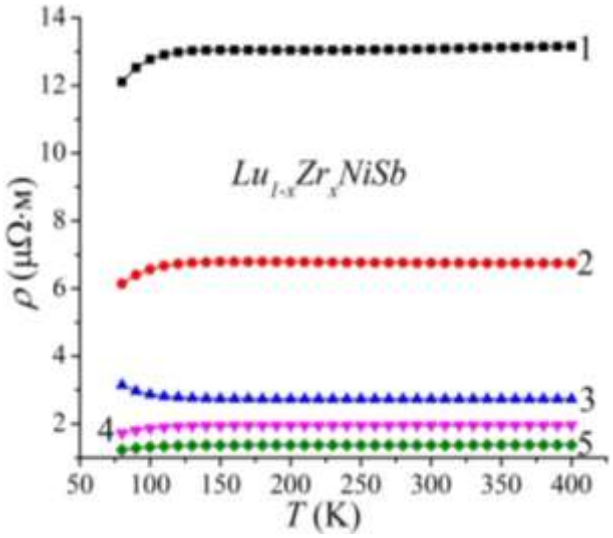

b)

Fig. 5. Temperature dependences of resistivity $\rho(T,x)$ $Lu_{1-x}Zr_xNiSb$:
a – experimental results, b – calculation;
1 – x = 0.01; 2 – x = 0.02; 3 – x = 0.05; 4 – x = 0.07; 5 – x = 0.1

Thus, from the above we can note the closeness of the results of experimental studies and calculations of changes in the values of the kinetic characteristics of the semiconductor solid solution $Lu_{1-x}Zr_xNiSb$ (Fig. 4 – 6). This is evidence of both the correctness of the experiment and the chosen method of modeling.

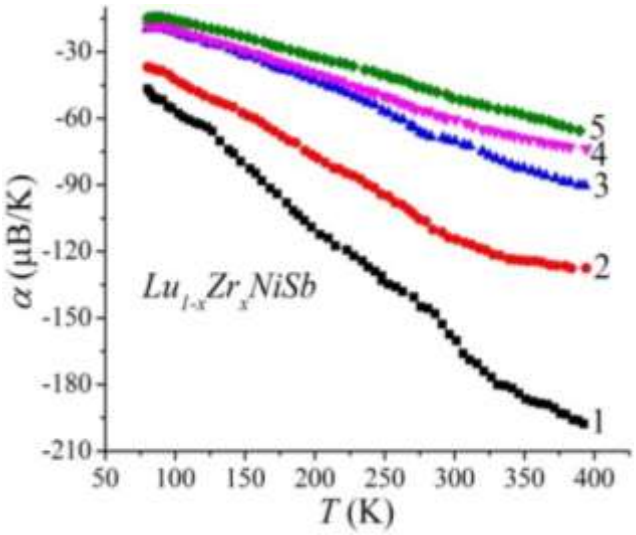

a)

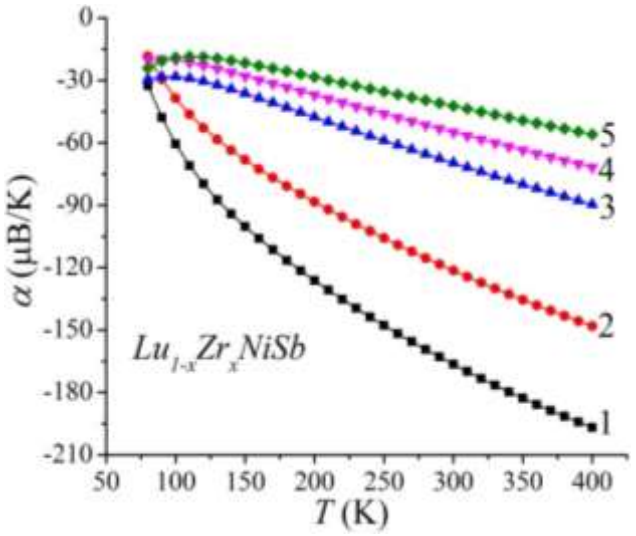

b)

Fig. 6. Temperature dependences of the thermopower coefficient α(*T,x*) *Lu1-xZrxNiSb: a – experimental results, b – calculation; 1 – x = 0.01; 2 – x = 0.02; 3 – x = 0.05; 4 – x = 0.07; 5 – x = 0.1*

The nature of the change in the values of the resistivity ρ(*x, T*) *Lu1-xZrxNiSb* at all temperatures turned out to be unexpected (Fig. 7*a*). It is known that if two types of electric current carriers are present in a semiconductor at the same time, then the maximum on the dependence ρ(*x, T*) indicates that the concentrations of the available ionized acceptors and donors are balanced. Available in Fig. 7*a*, the maximum on the dependence ρ(*x, T*) *Lu1-xZrxNiSb* on *x*≈0.01 has a different nature. After all, for *x* = 0 we have a semiconductor of *p*-type conductivity, when the Fermi level ε_F lies at a distance of 10.2 meV near the valence band ε_V. And at a concentration of *x* = 0.01 it is located deep in the conduction band ε_C and electrons are the main carriers. The same applies to the nature of the change in the values of the thermopower coefficient α(*T, x*) *Lu1-xZrxNiSb*, in particular, the available minimum at *x* ≈ 0.01 (Fig. 7*b*). It is correct to talk only about the increase in the values of ρ(*x, T*) and α(*x,T*) *Lu1-xZrxNiSb* at all

temperatures in the concentration range $0.01 \le x \le 0.10$ (Fig. 7*a*), when the Fermi level ε_F is located in the conduction band ε_C. And the reason for this behavior $\rho(x,T)$ and $\alpha(x,T)$ $Lu_{1-x}Zr_xNiSb$ is the increase in the concentration of free electrons and the density of states at the Fermi level ε_F. This is understandable, because *Zr* atoms, replacing *Lu*, generate structural defects of donor nature, which supply electrons to the semiconductor.

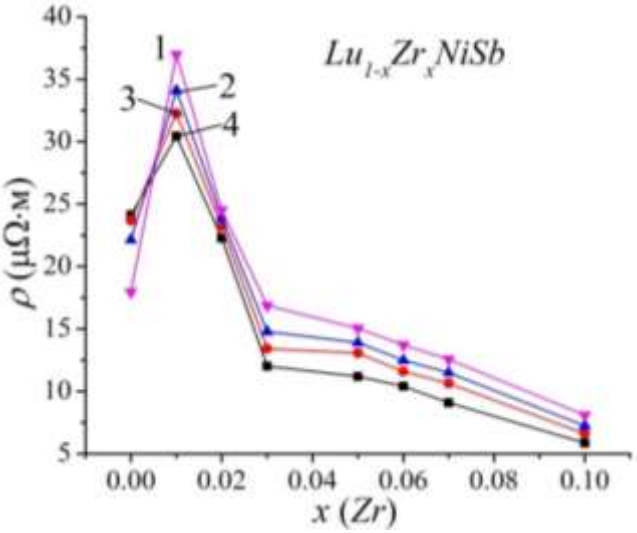

a)

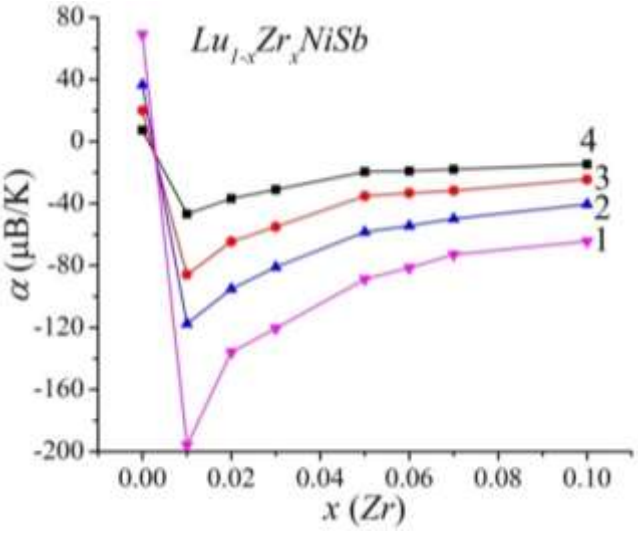

b)

Fig. 7. Change in the values of resistivity ρ(x,T) (a) and the thermopower coefficient α(T,x) (b) $Lu_{1-x}Zr_xNiSb$ at different temperatures: 1 – T = 380 K; 2 – T = 250 K; 3 – T = 160 K; 4 – T = 80 K

Extremely interesting and informative were the results of calculation from low-temperature activation regions of $\alpha(1/T)$ $Lu_{1-x}Zr_xNiSb$ dependences of activation energies $\varepsilon_1^{\alpha}(x)$ (Fig. 8*a*), the values of which are proportional to the amplitude of large-scale fluctuations in the zones of continuous energy in the

crystal space of charged centers, in particular, ionized acceptors and donors [14]. And the higher the degree of compensation of the semiconductor (the ratio of ionized acceptors and donors), the greater the distortion of the zones and the value of the modulation amplitude of the zones of continuous energies.

It should be noted at once that it is correct to analyze the behavior of the activation energy $\varepsilon_1^{\alpha}(x)$ $Lu_{1-x}Zr_xNiSb$ only at the concentration range $0.01 \le x \le 0.10$, when the conductivity of the semiconductor determines one type of basic carriers. After all, for $x = 0$ we have a semiconductor of hole type of conductivity, and for $0.01 \le x$ – electronic. From fig. 8*a*, it follows that at concentrations of $0.01 \le x \le 0.10$ the values of the activation energy $\varepsilon_1^{\alpha}(x)$ $Lu_{1-x}Zr_xNiSb$ rapidly decrease, indicating the predominance of the concentration of one type of electric current carrier over another. Since the main carriers of $Lu_{1-x}Zr_xNiSb$ current at $0.01 \le x$ are electrons and their concentration is much higher than that of holes, the ratio of donors to holes increases with increasing impurity concentration (the degree of compensation decreases).

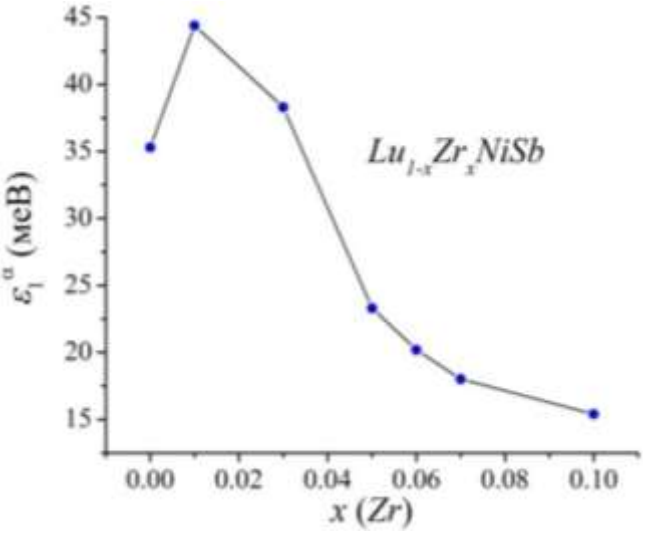

a)

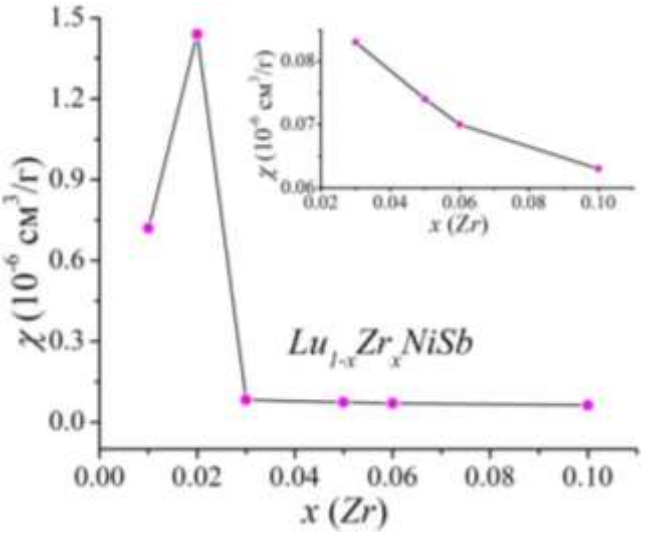

b)

Fig. 8. Change in the values of activation energy $\varepsilon_1^{\alpha}(x)$ (a) and specific magnetic susceptibility $\chi(x)$ (b) $Lu_{1-x}Zr_xNiSb$ for T = 293 K

In the classical case of doping, for example, a *p*-type semiconductor with a donor impurity, it first leads to the capture of free electrons by acceptors (ionization of acceptors) to concentrations when the number of acceptors corresponds to the number of ionized donors. At higher concentrations, when all acceptors are ionized, the donor electrons become collectivized (free) and participate in electrical conductivity. That is, first the electrons are captured by the acceptors present in the semiconductor [14]. In the case of $Lu_{1-x}Zr_xNiSb$, this compensation mechanism is absent.

The question of the reason for such nonclassical behavior of the kinetic characteristics of $Lu_{1-x}Zr_xNiSb$ seems logical. That is, what structural changes in $Lu_{1-x}Zr_xNiSb$ could have caused such a significant effect on the electronic system of the semiconductor, which is reflected in the above electrokinetic characteristics?

Recall that in the structure of *p-LuNiSb* there are vacancies at position 4*c* of *Ni* atoms, which generates structural defects of acceptor nature, and in the band gap ε_g appears the corresponding acceptor level (band) ε_A^1 [3, 6]. In addition, structural studies of $Lu_{1-x}Zr_xNiSb$ found that one of the reasons for the increase in the values of the period of cell $a(x)$ in the area of concentrations $x = 0 – 0.02$ (Fig. 1*b*) is the return to the 4*c* position of *Ni* atoms (elimination of vacancies). At the same time, position 4*c* generates structural defects of donor nature and eliminates structural defects of acceptor nature (namely, elimination of vacancies, not their ionization during electron capture). At the same time, the donor level (zone) ε_D^2 appears in the forbidden zone ε_g $Lu_{1-x}Zr_xNiSb$ and the corresponding acceptor level (zone) ε_A^1 disappears.

However, the simultaneous disappearance of acceptors and the activation of donor generation mechanisms, in particular when *Zr* atoms replace *Lu* atoms at position 4*a* and the return of *Ni* atoms to position 4*c*, cannot cause a giant concentration of donors to appear in the $Lu_{1-x}Zr_xNiSb$ semiconductor. the conduction band ε_C at the lowest concentration ($x = 0.01$). We can assume the existence of another, not described above, the mechanism of donor generation in $Lu_{1-x}Zr_xNiSb$, which is associated with changes in the concentration of Zr atoms.

Experimental studies of the magnetic susceptibility of $\chi(x)$ have shown that samples of both *LuNiSb* compounds and $Lu_{1-x}Zr_xNiSb$ solid solutions at all concentrations are Pauli paramagnetics (Fig. 8*b*). In this case, the synchrony of the behavior of the dependences of the resistivity $\rho(x,T)$ (Fig. 7*a*), the thermopower coefficient $\alpha(T,x)$ (Fig. 7*b*) and the magnetic susceptibility $\chi(x)$ (Fig. 8*b*), associated with a change in the density of states at the Fermi level ε_F.

Therefore, the study of a semiconductor solid solution of $Lu_{1-x}Zr_xNiSb$ obtained by doping a *LuNiSb* compound with *Zr* atoms by substituting Lu atoms in the crystallographic position 4*a* showed the complex nature of the impurity atoms entering the compound matrix when changes occur in several positions simultaneously. The first and most important step in modeling the electronic structure of $Lu_{1-x}Zr_xNiSb$, in particular the behavior of the Fermi level ε_F, is to understand the features of the spatial arrangement and electronic structure of the basic semiconductor *p-LuNiSb*. It is these features that determine the way in which impurity atoms enter the semiconductor matrix, which determines the formation of structural defects of different nature and the appearance in the forbidden zone of the corresponding energy levels..

Refinement of electronic and crystal structures of the basic *p-LuNiSb* semiconductor

If we take as a basis an ordered model of the crystal structure of the *LuNiSb* compound, in which all crystallographic positions are occupied by atoms according to the structural type of *MgAgAs* [5], then modeling of the electronic structure of *LuNiSb* shows that the compound is an *n*-type semiconductor (Fig. 9). Accordingly, the Fermi level ε_F (dashed line) lies near the conduction band ε_C, which in the experiment will give negative values of the thermopower coefficient $\alpha(T)$. However, this

simulation result does not agree with the results of experimental studies (Fig. 3*a*), where positive values of the thermopower coefficient α(*T*) were obtained.

The inconsistency of the results of experimental studies of the basic *p-LuNiSb* semiconductor and modeling of its electronic structure for an ordered model of the crystal structure indicates its disorder. Therefore, in the crystal structure of the compound *LuNiSb* there is a partial occupation of atoms of foreign positions, and it is also possible to have vacancies in different crystallographic positions. After all, in the case of doping the *LuNiSb* with impurity atoms, the presence of vacancies will determine the ways of formation of structural defects and energy levels in the band gap ε_g. That is why it is important to establish the features of the crystal structure of the *p-LuNiSb* semiconductor.

To clarify the crystal structure of the compound *LuNiSb*, as close as possible to the results of experimental measurements (Fig. 3*a*), modeling of its electronic structure for different variants of the spatial arrangement of atoms and the availability of vacancies. In Fig. 9 shows the distribution of the DOS electron density for an ordered model of the crystal structure of the *LuNiSb* compound (all atoms occupy their own positions), but the crystallographic positions of 4*a Lu* atoms and 4*c Ni* atoms contain a certain number of vacancies.

Thus, in the hypothetical compound $Lu_{0.99}NiSb$ the Fermi level ε_F will change its position and is located at the edge of the valence band ε_V: the dielectric-metal conductivity transition will occur (Fig. 9), and free holes become the main current carriers. The location of the Fermi level ε_F near the edge of the valence band ε_V or in the band itself is understandable, because the absence of the *Lu* atom at position 4*a* generates a structural defect of acceptor nature and the corresponding acceptor level (band). In this experiment we will have positive values of the thermopower coefficient α(*T*) $Lu_{0.99}NiSb$, and the intersection of the Fermi level ε_F and the valence band ε_V will change the conductivity from activation to metallic: the values of resistivity ρ will increase with temperature.

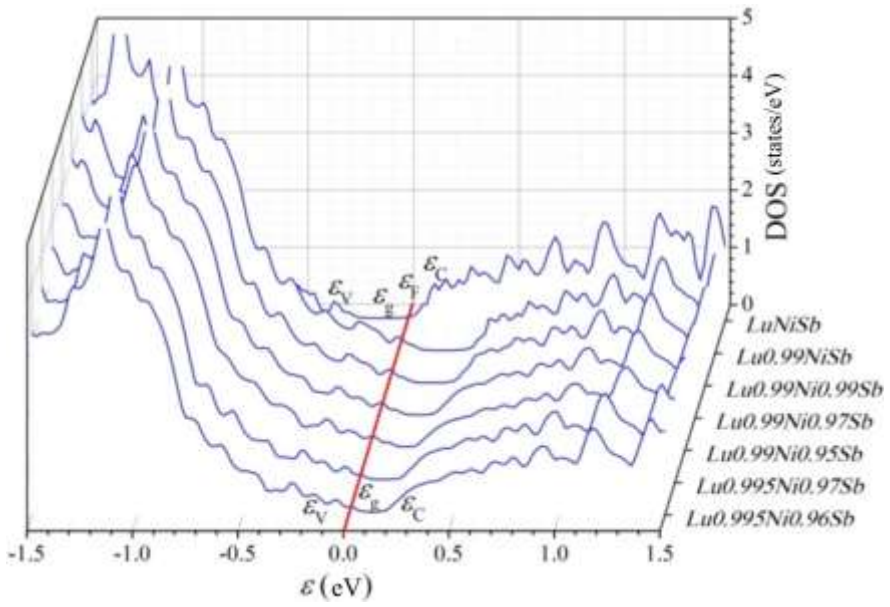

Fig. 9. Calculation of the density distribution of electronic states of DOS for different employment options of the crystallographic positions of the compound LuNiSb

Such simulation results with respect to the type of main electric current carriers correspond to the experimental results (Fig. 3*a*). However, experimental studies have shown that the temperature dependences of the resistivity ρ(*T*) of *LuNiSb* contain high- and low-temperature activation regions,

indicating the activation of holes from the Fermi level ε_F to the edge of the valence band ε_V. Therefore, the Fermi level ε_F in the real crystal is located in the band gap ε_g of the semiconductor, and not the edge of the valence band ε_V, as shown by the simulation results for the case $Lu_{0.99}NiSb$.

The most acceptable results of experimental studies are the model of the electronic structure of the compound *LuNiSb*, which assumes the presence of vacancies in the crystallographic positions of 4*a* *Lu* atoms (~0.005) and 4*c* Ni atoms (~0.04) (Fig. 9). In this model $Lu_{0.995}Ni_{0.96}Sb$ the spatial arrangement of atoms and the presence of vacancies at positions 4*a* and 4*c*, the compound is a hole-type semiconductor semiconductor in which the Fermi level ε_F is located in the band gap near the edge of the valence band ε_V. Under this model of the electronic structure of *p-LuNiSb* on the temperature dependences of the resistivity $\rho(T)$ will be present high- and low-temperature activation sites, and the value of the thermopower coefficient $\alpha(T)$ corresponds to the results of the experiment (Fig. 3*a*).

Thus, doping of the *LuNiSb* semiconductor with donor *Zr* impurities introduced into the structure by substituting Lu atoms at position 4*a* revealed defects of acceptor nature in the structure of the base compound as a result of vacancies at crystallographic positions 4*a* and 4*c* of *Lu* and *Ni* atoms, respectively, the corresponding acceptor levels (zones). The ratio of the concentrations of donor and acceptor levels present in the structure of the *LuNiSb* compound determines the location of the Fermi level ε_F in the semiconductor, and its doping with *Zr* donors will change the mechanisms and type of conductivity $Lu_{1-x}Zr_xNiSb$.

Conclusions

The result of a comprehensive study of the crystal and electronic structures, thermodynamic, kinetic, energy and magnetic properties of the thermoelectric material $Lu_{1-x}Zr_xNiSb$ is the establishment of the nature of structural defects of donor and acceptor nature. It is shown that the structure of the basic compound *LuNiSb* has defects of acceptor nature as a result of vacancies in the crystallographic positions 4*a* and 4*c* of *Lu* and *Ni* atoms, respectively, which gave rise to acceptor levels (zones) in the band gap ε_g. Introduction of *Zr* impurity atoms into the structure of the *LuNiSb* compound by substitution of *Lu* atoms in position 4*a* generates structural defects of donor nature with simultaneous elimination of vacancies in positions 4*a* and 4*c* of *Lu* and *Ni* atoms, respectively (acceptor levels). The ratio of the concentrations of available donors and acceptors determines the location of the Fermi level ε_F and the conduction mechanisms in $Lu_{1-x}Zr_xNiSb$. The investigated solid solution $Lu_{1-x}Zr_xNiSb$ is a promising thermoelectric material. The investigated solid solution $Lu_{1-x}Zr_xNiSb$ is a promising thermoelectric material, but requires additional research.

References

1. Karla I., Pierre J., Skolozdra R.V. (1998). Physical properties and giant magnetoresistance in *RNiSb* compounds. *J. Alloys Compd*., 265, 42–48. (DOI: https://doi.org/10.1016/S0925-8388(97)00419-2).
2. Romaka V.V., Romaka L., Horyn A., Rogl P., Stadnyk Yu., Melnychenko N., Orlovskyy M., Krayovskyy V. (2016). Peculiarities of thermoelectric half-Heusler phase formation in *Gd-Ni-Sb* and *Lu-Ni-Sb* ternary systems. *J. Solid State Chem*., 239, 145–152. (DOI: https://doi.org/10.1016/j.jssc.2016.04.029).
3. Romaka V.A, Stadnyk Yu., Romaka L., Krayovskyy V., Klyzub P., Pashkevych V., Horyn A., Garanyuk P. (2021). Synthesis and Electrical Transport Properties of $Er_{1-x}Sc_xNiSb$ Semiconducting Solid Solution. *J. Phys. and Chem. Sol. State*, 22(1), 146-152. (DOI: 10.15330/pcss.22.1.146-152).
4. Stadnyk Yu., Romaka V.A, Horyn A., Romaka V.V., Romaka L., Klyzub P., Pashkevych V., Garanyuk P. Modeling of Structural and Energetic Parameters of $p\text{-}Er_{1-x}Sc_xNiSb$ Semiconductor.

J. Phys. and Chem. Sol. State, 22(3), 509-515. (DOI: 10.15330/pcss.22.3.509-515).

5. Romaka V.V., Romaka L.P., Krayovskyy V.Ya., Stadnyk Yu.V. (2015). *Stanidy ridkisnozemelnykh ta perekhidnykh metaliv* [*Stannides of rare earth and transition metals*] Lviv: Lvivska Polytechnika [in Ukrainian].
6. Romaka V.A., Stadnyk Yu.V., Krayovskyy V.Ya., Romaka L.P., Guk O.P., Romaka V.V., Mykyuchuk M.M., Horyn A.M. (2020). *Novitni termochutlyvi materialy ta peretvoriuvachi temperatury* [*New thermosensitive materials and temperature converters*]. Lviv, Lvivska Polytechnika [in Ukrainian].
7. Anatychuk L.I. (1979). *Termoelementy i termoelectricheskiie ustroistva. Spravochnik.* [*Thermoelements and thermoelectric devices. Reference book*]. Kyiv: Naukova dumka [in Russian].
8. Roisnel T., Rodriguez-Carvajal J. (2001). WinPLOTR: a windows tool for powder diffraction patterns analysis. *Mater. Sci. Forum*, Proc. EPDIC7 378–381, 118–123.
9. Akai H. (1989). Fast Korringa-Kohn-Rostoker coherent potential approximation and its application to FCC *Ni-Fe* systems. *J. Phys.: Condens. Matter*., 1, 8045–8063.
10. Moruzzi V.L., Janak J.F., Williams A.R. (1978). *Calculated electronic properties of metals.* NY: Pergamon Press.
11. Savrasov S.Y. (1996). Linear-response theory and lattice dynamics: A muffin-tin-orbital approach. *Phys. Rev. B*, 54(23), 16470–16486.
12. Momma K., Izumi F. (2008). VESTA: a three-dimensional visualization system for electronic and structural analysis. *J. Appl. Crystallogr*., 41, 653–658.
13. Bader R.F.W. (1994). *Atoms in Molecules: A Quantum Theory*. Oxford: Clarendon press.
14. Shklovskii B.I. and Efros A.L. (1984). *Electronic properties of doped semiconductors* NY: Springer; (1979) Moscow: Nauka.
15. Mott N.F., Davis E.A. (1979). *Electron processes in non-crystalline materials.* Oxford: Clarendon Press.

Submitted 12.03.2021

Ромака В.А. *докт. техн.наук, професор*[1]**,**
Стадник Ю.В. *канд. хім. наук*[2]**,**
Ромака Л.П. *канд. хім. наук*[2]**,**
Пашкевич В.З. *канд. техн. наук, доцент*[1]**,**
Ромака В.В. *докт. техн.наук,*
канд. хім. наук, професор[3]**,**
Горинь А.М. *канд. хім. наук*[2]**,**
Демченко П.Ю. *канд. хім. наук*[2]

[1]Національний університет "Львівська політехніка", вул. С. Бандери,
12, Львів, 79013, Україна, *e-mail: vromaka@polynet.lviv.ua*;
[2]Львівський національний університет ім. І. Франка, вул. Кирила і Мефодія,
6, Львів, 79005, Україна, *e-mail: lyubov.romaka@lnu.edu.ua*;
[3]Дрезденський технічний університет, Бергштрассе 66,
Дрезден, 01069 Німеччина, *e-mail: vromakal@gmail.com*

ДОСЛІДЖЕННЯ СТРУКТУРНИХ, ТЕРМОДИНАМІЧНИХ, ЕНЕРГЕТИЧНИХ, КІНЕТИЧНИХ ТА МАГНІТНИХ ВЛАСТИВОСТЕЙ ТЕРМОЕЛЕКТРИЧНОГО МАТЕРІАЛУ $Lu_{1-x}Zr_xNiSb$

Досліджено кристалічну та електронну структури, термодинамічні, кінетичні, енергетичні та магнітні властивості термоелектричного матеріалу $Lu_{1-x}Zr_xNiSb$ у діапазонах: T = 80–400 K, x = 0–0.10. Встановлено механізми одночасного генерування структурних дефектів акцепторної та донорної природи. Показано, що у структурі базової сполуки LuNiSb присутні дефекти акцепторної природи як результат наявності вакансій у кристалографічних позиціях 4a та 4c атомів Lu та Ni відповідно, що обумовило появу у забороненій зоні ε_g акцепторних рівнів (зон). Уведення до структури сполуки LuNiSb домішкових атомів Zr шляхом заміщення у позиції 4a атомів Lu генерує структурні дефекти донорної природи з одночасною ліквідацією вакансій у позиціях 4a та 4c атомів Lu та Ni відповідно (акцепторних рівнів). Співвідношення концентрацій наявних дефектів донорної та акцепторної природи визначає у $Lu_{1-x}Zr_xNiSb$ розташування рівня Фермі ε_F та механізми провідності. Досліджений твердий розчин $Lu_{1-x}Zr_xNiSb$ є перспективним термоелектричним матеріалом. Бібл. 15, рис. 9.
Ключові слова: електронна структура, електроопір, коефіцієнт термоЕРС.

Ромака В.А. *докт. техн.наук, профессор*[1],
Стадник Ю.В. *канд. хим. наук*[2],
Ромака Л.П. *канд. хим. наук*[2],
Пашкевич В.З. *канд. техн. наук, доцент*[1],
Ромака В.В. *докт. техн.наук, канд. хим. наук, профессор*[3],
Горынь А.М. *канд. хим. наук*[2],
Демченко П.Ю. *канд. хим. наук*[2]

[1]Национальный университет "Львовская политехника", ул. С. Бандеры,
12, Львов, 79013, Украина, *e-mail: vromaka@polynet.lviv.ua*;
[2]Львовский национальный университет им. И. Франко, ул. Кирилла и Мефодия,
6, Львов, 79005, Украина, *e-mail: lyubov.romaka@lnu.edu.ua*;
[3]Дрезденский технический университет, Бергштрассе 66, Дрезден,
01069 Германия, *e-mail: vromakal@gmail.com*

ИССЛЕДОВАНИЕ СТРУКТУРНЫХ, ТЕРМОДИНАМИЧЕСКИХ, ЭНЕРГЕТИЧЕСКИХ, КИНЕТИЧЕСКИХ И МАГНИТНЫХ СВОЙСТВА ТЕРМОЭЛЕКТРИЧЕСКИХ МАТЕРИАЛОВ $Lu_{1-x}Zr_xNiSb$

Исследованы кристаллическая и электронная структуры, термодинамические, кинетические, энергетические и магнитные свойства термоэлектрического материала $Lu_{1-x}Zr_xNiSb$ в диапазонах: T = 80-400 K, x = 0-0.10.Установлены механизмы одновременного генерирования структурных дефектов акцепторной и донорной природы. Показано, что в структуре базового соединения LuNiSb присутствуют дефекты акцепторной природы как результат наличия вакансий в кристаллографических позициях 4a и 4c атомов Lu и Ni соответственно, что обусловило появление в запрещенной зоне ε_g акцепторных уровней (зон). Введение в структуру соединения LuNiSb примесных атомов Zr путем замещения в позиции 4a атомов Lu генерирует структурные дефекты донорной природы с одновременной ликвидацией вакансий в позициях 4a и 4c атомов Lu и Ni соответственно (акцепторных уровней). Соотношение концентраций имеющихся дефектов донорной и акцепторной природы определяет в $Lu_{1-x}Zr_xNiSb$ положение уровня Ферми ε_F и механизмы проводимости. Исследованный твердый раствор $Lu_{1-x}Zr_xNiSb$ является перспективным термоэлектрическим материалом. Библ. 15, рис. 9.

Ключевые слова: Электронная структура, электросопротивление, коэффициент термоЭДС.

References

1. Karla I., Pierre J., Skolozdra R.V. (1998). Physical properties and giant magnetoresistance in *RNiSb* compounds. *J. Alloys Compd*., 265, 42–48. (DOI: https://doi.org/10.1016/S0925-8388(97)00419-2).
2. Romaka V.V., Romaka L., Horyn A., Rogl P., Stadnyk Yu., Melnychenko N., Orlovskyy M., Krayovskyy V. (2016). Peculiarities of thermoelectric half-Heusler phase formation in *Gd-Ni-Sb* and *Lu-Ni-Sb* ternary systems. *J. Solid State Chem*., 239, 145–152. (DOI: https://doi.org/10.1016/j.jssc.2016.04.029).
3. Romaka V.A, Stadnyk Yu., Romaka L., Krayovskyy V., Klyzub P., Pashkevych V., Horyn A., Garanyuk P. (2021). Synthesis and Electrical Transport Properties of $Er_{1-x}Sc_xNiSb$ Semiconducting Solid Solution. *J. Phys. and Chem. Sol. State*, 22(1), 146-152. (DOI: 10.15330/pcss.22.1.146-152).
4. Stadnyk Yu., Romaka V.A, Horyn A., Romaka V.V., Romaka L., Klyzub P., Pashkevych V., Garanyuk P. Modeling of Structural and Energetic Parameters of $p\text{-}Er_{1-x}Sc_xNiSb$ Semiconductor. *J. Phys. and Chem. Sol. State*, 22(3), 509-515. (DOI: 10.15330/pcss.22.3.509-515).
5. Romaka V.V., Romaka L.P., Krayovskyy V.Ya., Stadnyk Yu.V. (2015). *Stanidy ridkisnozemelnykh ta perekhidnykh metaliv* [*Stannides of rare earth and transition metals*] Lviv: Lvivska Polytechnika [in Ukrainian].
6. Romaka V.A., Stadnyk Yu.V., Krayovskyy V.Ya., Romaka L.P., Guk O.P., Romaka V.V., Mykyuchuk M.M., Horyn A.M. (2020). *Novitni termochutlyvi materialy ta peretvoriuvachi temperatury* [*New thermosensitive materials and temperature converters*]. Lviv, Lvivska Polytechnika [in Ukrainian].
7. Anatychuk L.I. (1979). *Termoelementy i termoelectricheskiie ustroistva. Spravochnik.* [*Thermoelements and thermoelectric devices*. *Reference book*]. Kyiv: Naukova dumka [in Russian].
8. Roisnel T., Rodriguez-Carvajal J. (2001). WinPLOTR: a windows tool for powder diffraction patterns analysis. *Mater. Sci. Forum*, Proc. EPDIC7 378–381, 118–123.
9. Akai H. (1989). Fast Korringa-Kohn-Rostoker coherent potential approximation and its application to FCC *Ni-Fe* systems. *J. Phys.: Condens. Matter*., 1, 8045–8063.

10. Moruzzi V.L., Janak J.F., Williams A.R. (1978). *Calculated electronic properties of metals.* NY: Pergamon Press.
11. Savrasov S.Y. (1996). Linear-response theory and lattice dynamics: A muffin-tin-orbital approach. *Phys. Rev. B,* 54(23), 16470–16486.
12. Momma K., Izumi F. (2008). VESTA: a three-dimensional visualization system for electronic and structural analysis. *J. Appl. Crystallogr*., 41, 653–658.
13. Bader R.F.W. (1994). *Atoms in Molecules: A Quantum Theory*. Oxford: Clarendon press.
14. Shklovskii B.I. and Efros A.L. (1984). *Electronic properties of doped semiconductors* NY: Springer; (1979) Moscow: Nauka.
15. Mott N.F., Davis E.A. (1979). *Electron processes in non-crystalline materials.* Oxford: Clarendon Press.

Submitted 12.03.2021